AD-A085 950 AIR FORCE GEOPHYSICS LAB HANSCOM AFB MA F/G 4/1
A METHOD TO PREDICT THE PARAMETERS OF A FULL SPECTRAL DISTRIBUT--ETC(U)
JAN 80 R O BERTHEL
UNCLASSIFIED AFGL-TR-80-0001 NL

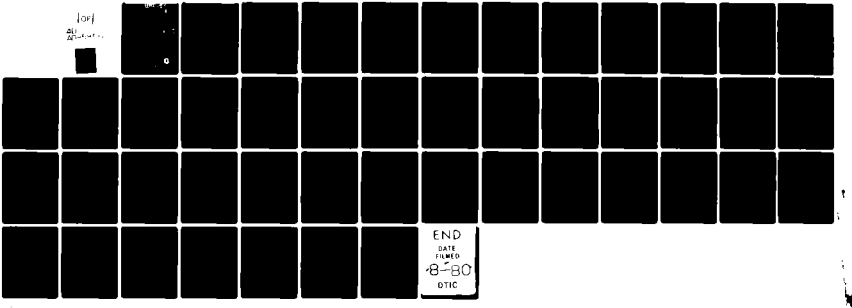

END
DATE FILMED
8-80
DTIC

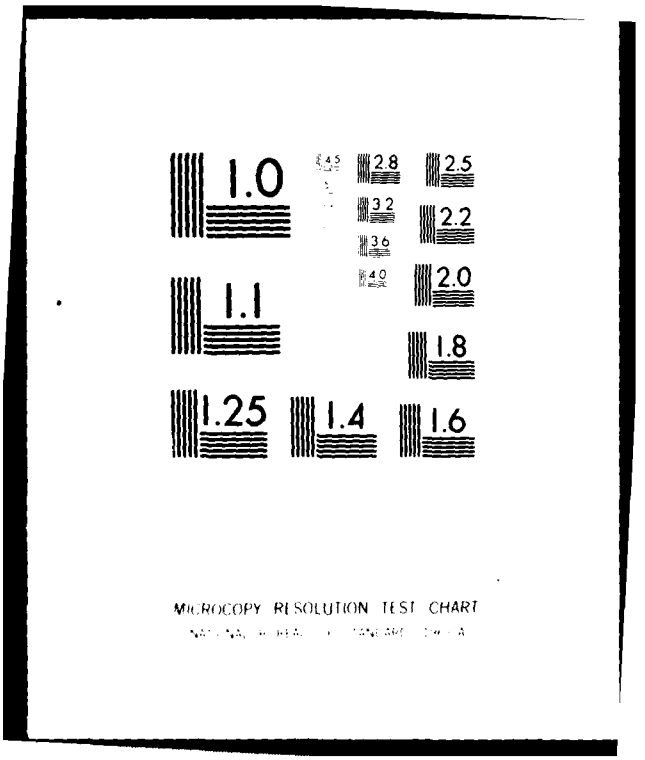
1.0
1.1
1.25
1.4
1.6
1.8
2.0
2.2
2.5
2.8
3.2
3.6
4.0
4.5
MICROCOPY RESOLUTION TEST CHART

A Method to Predict the Parameters of a Full Spectral Distribution From Instrumentally Truncated Data

ROBERT O. BERTHEL

7 January 1980

METEOROLOGY DIVISION PROJECT 6670
AIR FORCE GEOPHYSICS LABORATORY
HANSCOM AFB, MASSACHUSETTS 01731

AIR FORCE SYSTEMS COMMAND, USAF

This report has been reviewed by the ESD Information Office (OI) and is releasable to the National Technical Information Service (NTIS).

This technical report has been reviewed and is approved for publication.

FOR THE COMMANDER

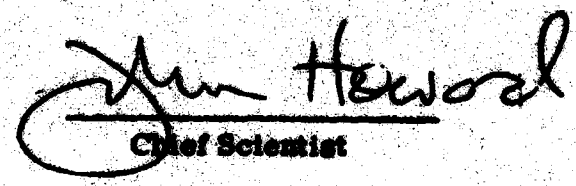

Chief Scientist

Qualified requestors may obtain additional copies from the Defense Documentation Center. All others should apply to the National Technical Information Service.

Unclassified

SECURITY CLASSIFICATION OF THIS PAGE (When Data Entered)

REPORT DOCUMENTATION PAGE	READ INSTRUCTIONS BEFORE COMPLETING FORM
1. REPORT NUMBER: AFGL-TR-80-0001	2. GOVT ACCESSION NO.: AD-A085 950
3. RECIPIENT'S CATALOG NUMBER:	
4. TITLE (and Subtitle): (6) A METHOD TO PREDICT THE PARAMETERS OF A FULL SPECTRAL DISTRIBUTION FROM INSTRUMENTALLY TRUNCATED DATA,	5. TYPE OF REPORT & PERIOD COVERED: Scientific. Interim.
	6. PERFORMING ORG. REPORT NUMBER: ERP No. 689
7. AUTHOR(s): (10) Robert O. Berthel	8. CONTRACT OR GRANT NUMBER(s): (12) 48
9. PERFORMING ORGANIZATION NAME AND ADDRESS: Air Force Geophysics Laboratory (LYC) Hanscom AFB Massachusetts 01731	10. PROGRAM ELEMENT, PROJECT, TASK AREA & WORK UNIT NUMBERS: 62101F 66701201; 61102F 2310G501; 63311F 627A0004
11. CONTROLLING OFFICE NAME AND ADDRESS: Air Force Geophysics Laboratory (LYC) Hanscom AFB Massachusetts 01731 (11)	12. REPORT DATE: 7 Jan 80 / 13. NUMBER OF PAGES: 48
14. MONITORING AGENCY NAME & ADDRESS(if different from Controlling Office)	15. SECURITY CLASS. (of this report): Unclassified; 15a. DECLASSIFICATION/DOWNGRADING SCHEDULE
16. DISTRIBUTION STATEMENT (of this Report): Approved for public release; distribution unlimited.	
17. DISTRIBUTION STATEMENT (of the abstract entered in Block 20, if different from Report): (16) 6670, 2310 (17) 11, 65	
18. SUPPLEMENTARY NOTES: (1) Environmental research papers,	
19. KEY WORDS (Continue on reverse side if necessary and identify by block number): Cloud physics; Hydrometeors; Particle distribution; Ice water content; Exponential distribution function (14) AFGL-TR-80-0001, AFGL-ERP-689	

20. ABSTRACT (Continue on reverse side if necessary and identify by block number)

This report describes a method of correcting measured hydrometeor distributions that are deficient in large-size particles because of instrument truncation. The corrective technique is developed with the analysis of experimental data and the application of the exponential-distribution function.

A discussion is presented on the power-function equations used to define hydrometeor environments and the application of the corrected spectra to these mathematical relationships.

DD FORM 1 JAN 73 1473 EDITION OF 1 NOV 65 IS OBSOLETE

Unclassified

SECURITY CLASSIFICATION OF THIS PAGE (When Data Entered)

409578

20. Abstract (Continued)

Equations are presented for the real-time analysis of truncated distributions to provide estimates of the non-truncated spectra.

Preface

The work presented in this report is a combination of the investigations pursued under three different in-house Work Units being conducted by the Cloud Physics Branch of AFGL. The measurement and determination of actual hydrometeor particle size distributions in the free atmosphere is a difficult basic research problem[1] and, as such, is being pursued under Task 2310G5, Cloud Physics, which is funded by the Air Force Office of Scientific Research (AFOSR). Data used to demonstrate the application of the method were obtained while the MC-130E and Branch members were supporting the SAMSO/ABRES ANT-2 mission at the Kwajalein Missile Range under the Advanced Development Project 627A, Weather Erosion Program. However, the majority of the effort reported herein was in the nature of exploratory development and was conducted under Task 667012, Cloud Microphysics.

Thanks are expressed to Dr. Arnold A. Barnes, Jr. and Mr. Vernon G. Plank for their valuable suggestions in the writing of this report.

1. Barnes, A.A., Jr. (1978) New cloud physics instrumentation requirements, Preprints, Fourth Symposium on Meteorological Observations and Instrumentation, American Meteorological Society, 264-268, AFGL-TR-0093, AD A053 235.

Contents

Illustrations

Illustrations

Tables

Tables

A Method to Predict the Parameters of a Full Spectral Distribution From Instrumentally Truncated Data

1. INTRODUCTION

The Air Force Geophysics Laboratory (AFGL) has equipped two aircraft, a Learjet and MC-130E, with a variety of instruments for measuring meteorological parameters. One use of the data acquired by these aircraft, either by themselves or in conjunction with ground-based radar, is to determine the liquid water content* of precipitable storm hydrometeors.

Contained within this specialized instrumentation are two types of Optical Array Probes manufactured by Particle Measuring Systems Inc. of Boulder, Colorado which are specifically designed to characterize and count the hydrometeors. A one-dimensional system (PMS 1-D) classifies these hydrometeors as to their physical size in one dimension and also measures the number density.[2] The two-dimensional instrument (PMS 2-D) provides an electronically-produced shadowgraph from which a two-dimensional size can be measured and type of precipitation particle can be inferred.[3]

Using the data from the 1-D, the liquid water content (M) of the sampled hydrometeors can be determined by

---

(Received for publication 7 January 1980)

*Liquid water content is defined in this report as the mass of water (rain or melted ice and snow) per unit atmospheric volume. Units are grams per cubic meter.

The references cited above will not be listed here. See References, page 41.

$$M = c \sum_{i=1}^{i=n} N_i D_i^3 \text{ g m}^{-3} \quad (1)$$

where N_i (m^{-3}) is the number concentration in a class having D_i (mm) as the mid-size diameter and

$$c = \frac{\pi}{6} \times 10^{-3} \rho_w \quad (2)$$

where ρ_w (g cm^{-3}) is the density of liquid water. The equivalent of the radar reflectivity (Z) can also be calculated from the same spectral data by

$$Z = \sum_{i=1}^{i=n} N_i D_i^6 \text{ mm}^6 \text{ m}^{-3} \quad . \quad (3)$$

In the case of an ice hydrometer, the D in the equations is taken as the equivalent melted diameter of the ice crystal and is defined by

$$D = \alpha \ell^{\beta} \quad (4)$$

where α and β are values that change in accord with the crystal type and ℓ is the physical dimension of the ice particle as measured by the PMS equipment.[4]

With the spectral information supplied by this instrument and the knowledge of crystal habit, the M and Z of the distribution can readily be determined, but a problem develops when some of the crystals grow to sizes that exceed the measuring capabilities of the instrument (3.601 mm for the 1-D system on the Lear and 5.402 mm for the system on the MC-130E). At this point, the spectral distribution is instrumentally truncated and the derived M and Z are valid only for the portion of the spectrum that was actually measured. The 2-D, on the other hand, is capable of recording parts of these large particles, and gives some knowledge as to physical size although the number density and size classification are not so well defined.

The purpose of this paper is to present a method of extrapolating the 1-D truncated distributions so that a reasonably accurate estimate of the total M and Z may be found and then describe how these corrected data may be conveniently

---

4. Cunningham, R.M. (1978) Analysis of particle spectral data from optical array (PMS) 1-D and 2-D sensors, Fourth Symposium on Meteorological Observations and Instrumentation, April 10-14, 1978, Denver, Colorado, Preprint Vol., pp 345-350.

incorporated in mathematical relationships that more closely represent the actual hydrometeor spectra.

2. EXTRAPOLATION OF A TRUNCATED DISTRIBUTION

The problems of extrapolating a distribution are twofold: Which method is to be used to extend the distribution beyond the upper truncation limit and what is the limit of the extension, or the determination of maximum particle size?

When addressing the first problem, it is logical to assume that the form of the number-density distribution will remain relatively constant beyond the physical size limitation. Therefore, the trend of the distribution should be established from the measured portion of the spectra.

Figures 1, 2 and 3 show the plotted number density vs the equivalent melted diameter for three separate passes taken on July 4, 1978 over the Kwajalein Atoll. All are measurements of hydrometeors classified as large snow, one sampled by the Lear and the others by the MC-130E, and all three have maximum physical sizes that are much larger than the I-D instruments are able to measure. (In all cases, the α in Eq. (4) is 0.4 and the β is 0.782). These distributions can be considered typical of the experimental data collected by AFGL in past years in that they exhibit a systematic decrease in the number density over the mid- to large-size diameter range. The figures demonstrate that a straight line, on a log-linear plot, can adequately describe the population for the major part (approximately 92 percent) of the total measured size range of each of the distributions. Deviation from the straight line occurs at or about the junction of the cloud and precipitation probes, with the cloud probe spectra following a line having a much steeper slope. The contributions of M and Z from the precipitation probe data (M_P and Z_P) constitute the majority of the measured values and indicate, at least in truncated situations, that the M_C and Z_C derived from the cloud probe spectra are minor contributions as shown in Table 1.

When the data from the precipitation probe of the 1-D instrument is considered by itself, it is apparent that the size distribution can be reasonably described by a function of exponential type which agrees with the observations made by numerous other investigators.[5, 6, 7, 8, 9, 10] Although this occurrence is evident in the vast majority of cases, an occasional sampling level will exhibt number-density distributions that do not conform to an exponential fit and can not be used in the following processes.

Because of the large number of references cited above, they will not be listed here. See References, page 41.

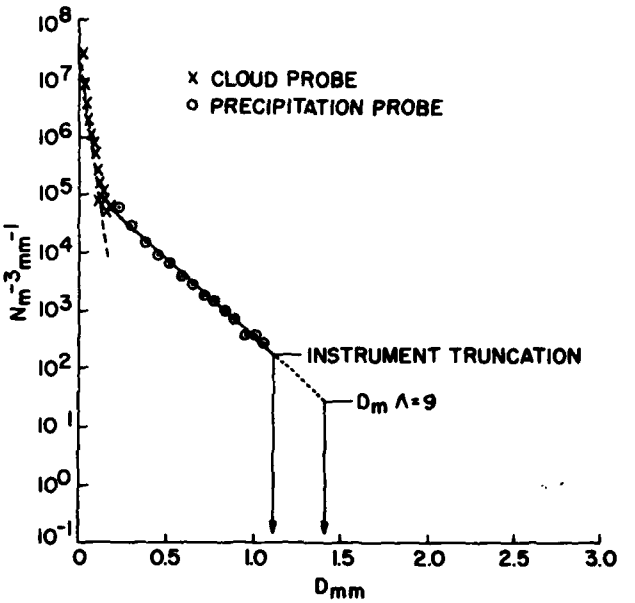

Figure 1. Number-Density Plot of Large Snow Hydrometeors as Recorded by the PMS 1-D on the Lear at an Altitude of 7 km over the Kwajalein Atoll on July 4, 1978 (99 sec av)

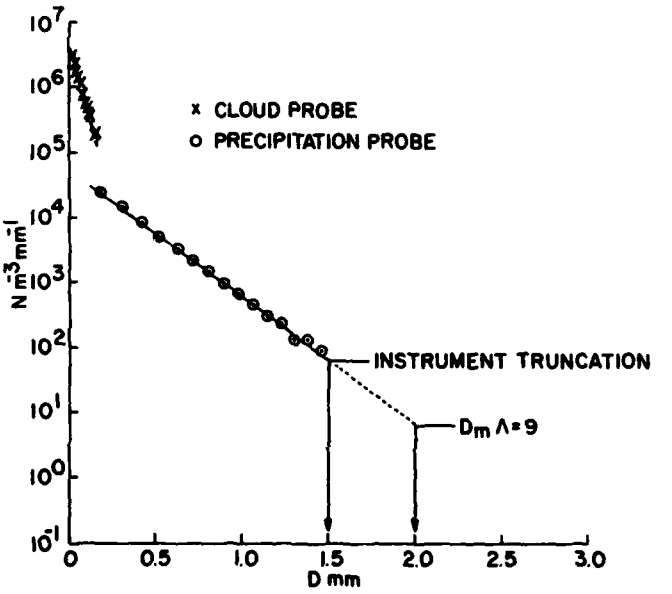

Figure 2. Number-Density Plot of Large Snow Hydrometeors as Recorded by the PMS 1-D on the MC-130E, Pass 3 at an Altitude of 5.1 km over the Kwajalein Atoll on July 4, 1978 (142 sec av)

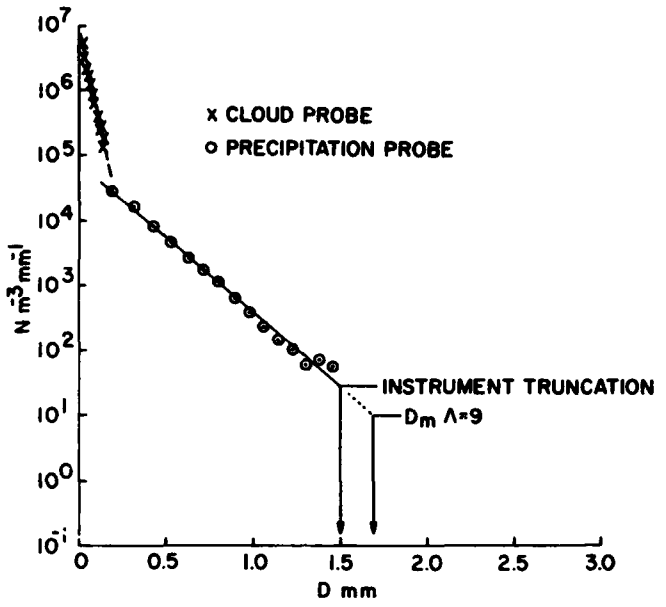

Figure 3. Number-Density Plot of Large Snow Hydrometeors as Recorded by the PMS 1-D on the MC-130E, Pass 5 at an Altitude of 6.6 km over the Kwajalein Atoll on July 4, 1978 (212 sec av)

An exponential size distribution specifies that the number concentration of the hydrometeors will decrease with increasing diameter as

$$N_D = N_o e^{-\Lambda D} \quad \text{No. m}^{-3}\ \text{mm}^{-1} \tag{5}$$

where N_o is the number per cubic meter per millimeter bandwidth and is a constant of the exponential-distribution function, Λ is number per millimeter bandwidth and is the slope of the number-density distribution and D is the drop diameter in millimeters or, in the case of ice hydrometeors, the equivalent melted diameter. The total number of hydrometeors in a population between a specific minimum (d) and a maximum diameter (D_M) is

$$N_T = \int_d^{D_M} N\, dD \quad \text{No. m}^{-3} \tag{6}$$

Table 1. Comparison of the M and Z Contributions Derived from the Measurements of the Cloud and Precipitation Probes of the PMS 1-D

	$M\ g\ m^{-3}$		Total $M\ g\ m^{-3}$	Percent from	
	Cloud Probe M_C	Precip. Probe M_P		Cloud Probe	Precip. Probe
Lear	0.0225	0.3279	0.3504	6.4	93.6
MC-130E Pass 3	0.0283	0.3824	0.4107	6.9	93.1
MC-130E Pass 5	0.0244	0.3062	0.3306	7.4	92.6
	$Z\ mm^6\ m^{-3}$		Total $Z\ mm^6\ m^{-3}$	Percent from	
	Cloud Probe Z_c	Precip. Probe Z_p		Cloud Probe	Precip. Probe
Lear	0.014	177.2	177.214	<0.01	>99.99
MC-130E Pass 3	0.054	544.1	544.154	0.01	99.99
Mc-130E Pass 5	0.040	336.4	336.440	0.01	99.99

or

$$N_T = \frac{N_o\, r_N}{\Lambda} \quad \text{No. } m^{-3} \tag{7}$$

where r_N is the truncation ratio of the number of hydrometeors contained within the d and D_M limits to the total N as

$$r_N = \frac{\int_d^{D_M} N\, dD}{\int_0^{\infty} N\, dD}, \tag{8}$$

or

$$r_N = e^{-d\Lambda} - e^{-D_M\Lambda}. \tag{9}$$

The hydrometeor liquid water content is distributed with diameter as

$$M_D = \frac{\pi}{6} \times 10^{-3} \rho_w N_o e^{-\Lambda D} \text{ g m}^{-3} \text{ mm}^{-1} \tag{10}$$

and the total M from d to D_M is

$$M = \int_d^{D_M} M_D \, dD \quad , \quad \text{g m}^{-3} \tag{11}$$

or

$$M = \frac{\pi \times 10^{-3} \rho_w N_o \Gamma(4) r_M}{6 \Lambda^4} \quad \text{g m}^{-3} \tag{12}$$

where $\Gamma(4)$ is the gamma function of 4 and r_M is the truncation ratio of the liquid water content contained within the d and D_M limits to the total M as

$$r_M = \frac{\int_d^{D_M} M_D \, dD}{\int_0^{\infty} M_D \, dD} \quad , \tag{13}$$

or

$$r_M = \frac{1}{6} \{ e^{-d\Lambda} [(d\Lambda)^3 + 3(d\Lambda)^2 + 6d\Lambda + 6] - e^{-D_M\Lambda} [(D_M\Lambda)^3 + 3(D_M\Lambda)^2 + 6D_M\Lambda + 6] \} \quad . \tag{14}$$

The radar-reflectivity distributed values for the same population are

$$Z_D = N_o D^6 e^{-\Lambda D} \text{ mm}^6 \text{ m}^{-3} \text{ mm}^{-1} \quad , \tag{15}$$

and the total Z within the d to D_M limits is

$$Z = \int_d^{D_M} Z_D \, dD \quad , \quad mm^6 \, m^{-3} \tag{16}$$

or

$$Z = \frac{N_o \, \Gamma(7) \, r_Z}{\Lambda^7} \quad mm^6 \, m^{-3} \tag{17}$$

where $\Gamma(7)$ is the gamma function of 7 and r_Z is the truncation ratio of the radar reflectivity contained within the d and D_M limits to the total Z as

$$r_Z = \frac{\int_d^{D_M} Z_D \, dD}{\int_0^{\infty} Z_D \, dD} \, , \tag{18}$$

or

$$r_Z = \frac{1}{720} \{ e^{-d\Lambda} [(d\Lambda)^6 + 6(d\Lambda)^5 + 30(d\Lambda)^4 + 120(d\Lambda)^3 + 360(d\Lambda)^2 + 720d\Lambda + 720]$$
$$- e^{-D_M\Lambda} [(D_M\Lambda)^6 + 6(D_M\Lambda)^5 + 30(D_M\Lambda)^4 + 120(D_M\Lambda)^3 + 360(D_M\Lambda)^2$$
$$+ 720(D_M\Lambda) + 720] \} \, . \tag{19}$$

When Eqs. (12) and (17) are solved for N_o they can be equated as

$$\frac{6 \, M \, \Lambda^4}{\pi \times 10^{-3} \, \rho_w \, \Gamma(4) \, r_M} = \frac{Z \, \Lambda^7}{\Gamma(7) \, r_Z} \tag{20}$$

and solved for Λ as

$$\Lambda = \left(\frac{6 \, M \, \Gamma(7) \, r_Z}{Z \pi \times 10^{-3} \, \rho_w \, \Gamma(4) \, r_M} \right)^{1/3} \quad mm^{-1} \, . \tag{21}$$

Substituting $\Gamma(4) = 6$, $\Gamma(7) = 720$ and $\rho_w = 1$ g cm^{-3}, Eq. (21) reduces to

$$\Lambda = 61.2 \left(\frac{M\, r_Z}{Z\, r_M} \right)^{1/3} \quad \text{mm}^{-1} \quad . \tag{22}$$

Since both r_M and r_Z incorporate Λ as a term (Eqs. (14) and (19)) then a "trial and error" method can be used to solve Eq. (22), whereby the value of Λ is adjusted until both sides of the equation are equal. Once Λ has been found, N_o can be determined using either Eq. (12) or (17) and the total number of particles may be calculated from Eq. (7).

If the M and Z derived from the truncated precipitation-probe measurements of the 1-D instrument are used in these equations with the appropriate diameter limits, where D_M now becomes the upper-truncation diameter D_T, then the distribution properties of the spectra can be described by a function of exponential type. The plotted exponentials of Figures 1, 2 and 3 (solid lines) were calculated in this manner where $d = 0.097$ mm and $D_T = 1.090$ mm for the Lear and $d = 0.133$ mm and $D_T = 1.496$ mm for the MC-130E data. It is apparent from these figures that the solid line representing the exponential number distribution establishes the trend of the spectrum. An estimation of that portion of the population missed because of instrument truncation can be made by extrapolating the line to some larger diameter.

The second part of the problem is the establishment of a new D_M value which reflects the maximum size of the nontruncated spectra. Past studies of exponential distributions conducted at AFGL[9] have shown that D_M can be related to Λ as

$$D_M \Lambda = C \tag{23}$$

when maximum particle sizes of known crystal habit are measured with the Aluminum Foil Hydrometeor Sampler[11] and/or the PMS 2-D and are converted to D_M values through Eq. (4). The normal range of C is between 9 and 12 and is dependent on crystal density and configuration. For the large-snow category of Figures 1, 2, and 3, C has the value of 9 and was determined from measurements of the PMS 2-D and the use of 0.4 for α and 0.782 for β in Eq. (4).

The maximum physical size recorded by the MC-130E 2-D for the flight passes plotted in Figures 2 and 3 were approximately 8 and 6.5 mm. The calculated D_M in Figure 2 is 2.0 mm which translates into a ℓ of 7.82 mm using the reverse

11. Church, J. F., Pocs, K. K., and Spatola, A. A. (1975) The Continuous Aluminum Foil Sampler; design operation, data analysis procedures, and operating instructions, Instrumentation Papers, No. 235, AFCRL-TR-75-0370, AD A019 630, 70 pp.

form of Eq. (4). The D_M of Figure 3 is 1.698 mm and the corresponding ℓ is 6.35 mm. Unfortunately, no comparison can be made for the Lear flight of Figure 1 since the 2-D instrument was inoperative during that time period.

The good agreement between the exponential number-density fit and the D_M assumption with the experimental results give an added degree of confidence for the determination of the parameters from a predicted, full distribution. Since N_o and Λ are known and a D_M has been established, the estimated values of M and Z can be determined by finding the M and Z contribution from the extrapolated part of the distribution (dotted line in Figures 1, 2 and 3) and adding them to the measured values as

$$M_E = M_P + \Delta M \quad g\ m^{-3} \tag{24}$$

and

$$Z_E = Z_P + \Delta Z \quad mm^6\ m^{-3} \tag{25}$$

where M_E and Z_E are the estimated liquid water content and radar reflectivity, M_P and Z_P are the values derived from the precipitation-probe measurements and ΔM and ΔZ are the contributions from the extrapolated D_T to D_M portion.

The equations for M_E and Z_E thus become

$$M_E = \int_d^{D_T} M_D\, dD + \int_{D_T}^{D_M} D_D\, dD \quad g\ m^{-3} \tag{26}$$

and

$$Z_E = \int_d^{D_T} Z_D\, dD + \int_{D_T}^{D_M} Z_D\, dD \quad mm^6\ m^{-3} \quad . \tag{27}$$

Since both first terms are known quantities, the solving of these equations becomes a two-part process where M_P and Z_P are used in Eq. (22) to determine the Λ of the exponential function which, in turn, is used in either Eq. (12) or (17) to find N_o. These parameters are then incorporated into the second term of Eqs. (26) and (27) to find ΔM and ΔZ.

Table 2 lists the M_P and Z_P that were derived from the measurements from the precipitation probe for the three sample passes compared with the estimated M_E and Z_E from the extrapolated spectra.

Table 2. Comparison of Precipitation Probe Data (M_P, Z_P) with the Estimated Values (M_E, Z_E) Determined from the Extrapolated Distributions

	M_P g m^{-3}	M_E g m^{-3}	Factor M_E/M_P	Z_P mm^6 m^{-3}	Z_E mm^6 m^{-3}	Factor Z_E/Z_P
Lear	0.3279	0.3533	1.077	177.2	268.3	1.514
MC-130E Pass 3	0.3824	0.4144	1.084	544.1	845.5	1.554
MC-130E Pass 5	0.3062	0.3137	1.024	336.4	393.6	1.170

In these three samples the increase, as a result of extrapolation, was only in the order of ~2 to 8 percent in M but ~17 to 55 percent in Z.

Although the amount of M and Z missed because of instrument truncation could vary considerably in different situations, it is clear from these results that it is the Z-parameter which shows the largest degradation. In the case of a slightly truncated distribution, the measured M may be an accepted value, but if the sampled hydrometeors are to be defined in a relationship of aircraft-measured M and Z, then new estimated values of Z have to be incorporated.

3. REGRESSION ANALYSIS OF MULTI-SAMPLE TRUNCATED AIRCRAFT DATA

In the normal analytical procedure used at AFGL, the multi-sample spectral data, acquired by the Lear and MC-130E along particular flight paths through cloud and storm situations, are used to obtain power-function equations that mathematically define hydrometeor environments.[8, 9, 12, 13, 14, 15, 16] This is done by the conventional method of cross-plotting the logarithmic values of M and Z from the multiple, individual samples. The least square analysis of this field of data points determines the line of best fit and provides the coefficient and exponent of the power-function regression equation. The ultimate goal is to relate M and Z in a regression relationship as

$$M = a Z^b \tag{28}$$

Because of the large number of references cited above, they will not be listed here. See References, page 41.

so that the liquid water content of a specific hydrometeor region can be calculated from a given radar reflectivity.

Two methods have been employed in past work to acquire M-Z information; one is the regression of the dependent variables of aircraft derived M_A versus Z_A and the other is the regression of the independent variables of M_A versus the radar-measured Z_R. Since the aircraft-spectral M and Z values are highly dependent upon the α and β in the ℓ to D conversion (Eq. (4)) and are also susceptible to instrument truncation effects, the first method has an inherent uncertainty in both of the values being correlated. Using the Z_R in place of the Z_A in the correlation removes these particular uncertainties from one parameter of the analysis since Z_R does not require a prior knowledge of α and β and, of course, is not limited to the measuring range of the 1-D instruments. Another benefit of using Z_R is the ability to sample the defined region during periods when the aircraft must be temporarily absent.

Studies have been conducted at AFGL on the variability of the spectral M_A and Z_A caused by an incomplete knowledge of the α and β terms of the ℓ to D conversion. For example, if the aircraft were to sample a homogeneous environment of pristine-crystal type and the α and β of Eq. (4) were precisely known, then the measured radar reflectivity (Z_R) should equal or very closely approximate the Z_A calculated from the aircraft data. Ideal conditions such as this are seldom, if ever, found in storm situations and usually the crystal mixes are so varied that the α and β is normally determined from the predominant type. The result is that Z_A and Z_R do not always closely agree; thus the liquid water content derived from the aircraft measurements (M_A) is not always the true M of the sample. It has been demonstrated that by using a spectral parameter k in the regression analysis, where k is defined as

$$k = M_A / \sqrt{Z_A} \quad g\ mm^{-3}\ m^{-1.5} \tag{29}$$

that the uncertainty effect of the ℓ to D relationship of Eq. (4) is minimized when deriving the M of a sample.[9, 16]

The correlation of k with the radar values is given by

$$k = a_1 Z_R^{b_1} \tag{30}$$

and is related to the M of the sample by

$$M = a_1 Z_R^{0.5+b_1} \quad . \tag{31}$$

The aircraft values themselves can also be expressed as

$$k = a_2 Z_A^{b_2} \tag{32}$$

and

$$M = a_2 Z_A^{0.5+b_2} \quad . \tag{33}$$

If the aircraft data used in Eqs. (29) through (33) are taken from the precipitation probe only, as in the following discussion, then the subscript "A" should be replaced with a "P" to more accurately describe the process. "A" will then refer to the combined values from both the cloud and precipitation probes.

When the aircraft spectral data used in these regression analyses stem from instrumentally-truncated samples, then it is apparent that the data must be corrected or compensated to take into account the effects of the truncation. The correction, when applied to the two regression methods, will display a similar effect on both of the k-Z correlations even though both parameters of the k_P-Z_P regression will be altered by the compensation and only the aircraft k-values in the k_P-Z_R regression will be affected. These two regression cases will be considered separately in the following discussion and the methods that may be used to correct them for the effects of truncation will be described.

An example of the k_P-Z_P correlation is plotted in Figure 4 and shows the 53 data points (4-second averages) of the precipitation-probe measurements from the MC-130E, pass 5 (Figure 3) scattered about the regression line. Any k_P-Z_P relationship of this nature will allow a corresponding value of k_P to be calculated for any given value of Z_P.

If some or all of the sampled distributions are instrumentally truncated, as in the example, the analysis (Eqs. (32) and (33)) is still valid for that specified limited situation but does not reflect the condition that actually exists. One method of correcting this regression is to use the M_P and Z_P of each individual truncated distribution in Eq. (22) and estimate a new M_E and Z_E as outlined in Section 2. New regressions can then be calculated based on the estimated parameters

$$k_E = a_3 Z_E^{b_3} \tag{34}$$

and

$$M_E = a_3 Z_E^{0.5+b_3} \tag{35}$$

as shown in Figure 5.

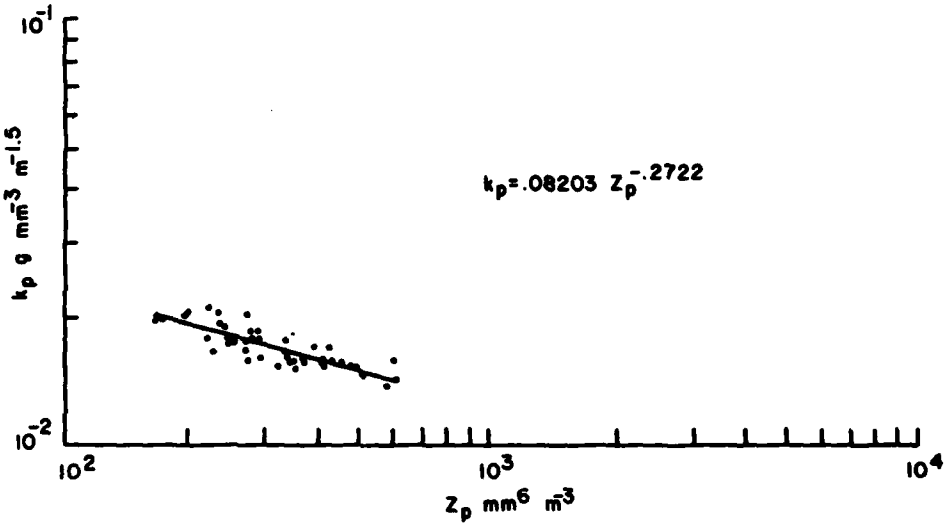

Figure 4. The k_P-Z_P Regression of the 53 Truncated Data Points (4-Second Averages) from the MC-130E, Pass 5

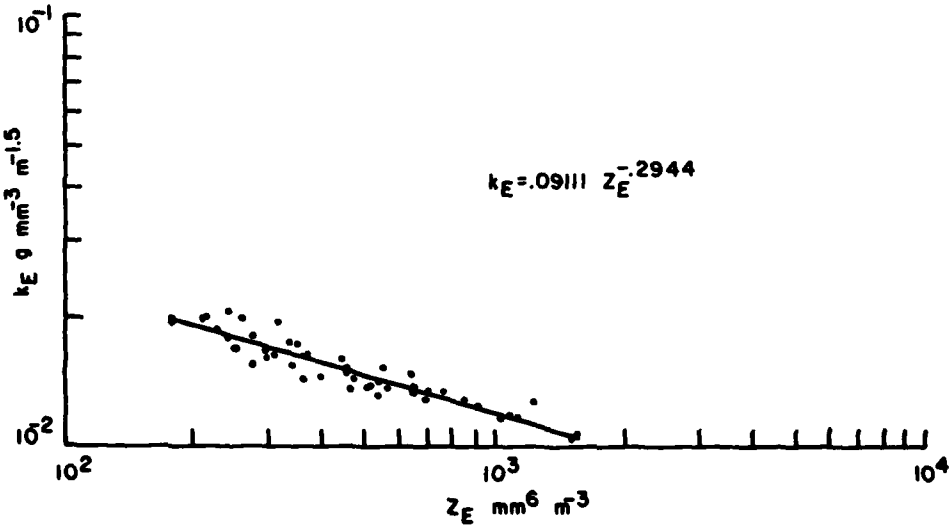

Figure 5. The k_E-Z_E Regression of the 53 Extrapolated Data Points from the MC-130E, Pass 5

This procedure, of course, is valid only when the multi-sample, averaging time-interval of the spectra is long enough and the data are of sufficient quality to insure that the individual distributions are of exponential form. As a check of this sample meeting these criteria, six randomly-chosen distributions from the total of 53 are plotted in Figure 6. When compared with the pass average plot (Figure 3), it is evident that the much shorter averaging time-interval causes an increase in the variability of the number density about the exponential slope although each of the six cases can still be reasonably described by an exponential function.

The method of regressing the estimated parameters from the extrapolation of each individual point (Figure 5) displays a more negative slope, which is as expected, when one reflects upon the changes that result from extrapolation.

It may be helpful, at this point, to review the changes that will occur when the extrapolation process is used and to illustrate in a simple diagram the expected effects of these corrections.

Figure 7 describes two k_P-Z_P regression lines (positive and negative) which are formed from five truncated distributions (open circles). In Section 2 it was shown that the number-density plot of an instrumentally truncated distribution, when extrapolated to a new $D_M\Lambda$ limit, will have a much larger increase in Z then in M since M varies with diameter to the third power (Eq. (1)) and Z varies with diameter to the six power (Eq. (3)). Also, when considering a distribution with a particular exponential slope, the larger the M and Z in the truncated distribution the larger the change will be upon extrapolation. Since the k-parameter is defined as M divided by the square root of Z (Eq. (29)) then it follows that k will decrease as a result of extrapolation and will also show larger changes in the more densely populated cases.

The X's in Figure 7 represent the estimated k_E and Z_E values that will result from correcting each truncated distribution and show the decrease in k along with the increase in Z for each compensated point. The resulting changes in both the positive and negative regression lines are similar, in that they both exhibit a more negative slope because of the corrections.

The method of extrapolating each individual distribution (Figure 5) gives satisfactory results but, since it involves so many extrapolations (one for each of the multiple samples), it becomes a long complicated process and it is obvious that a simpler and quicker procedure is needed.

A regression line calculated from truncated data, such as in Figure 4, represents the best straight-line relationship of k_P and Z_P as dictated by the hydrometeors sampled during the pass. The regression line of Figure 5 is, correspondingly, the best relationship obtained by the regression of the extrapolated data points. Transformation from the truncated to the non-truncated case may, therefore, be considered in the context of change in the lines of best fit rather than changes in

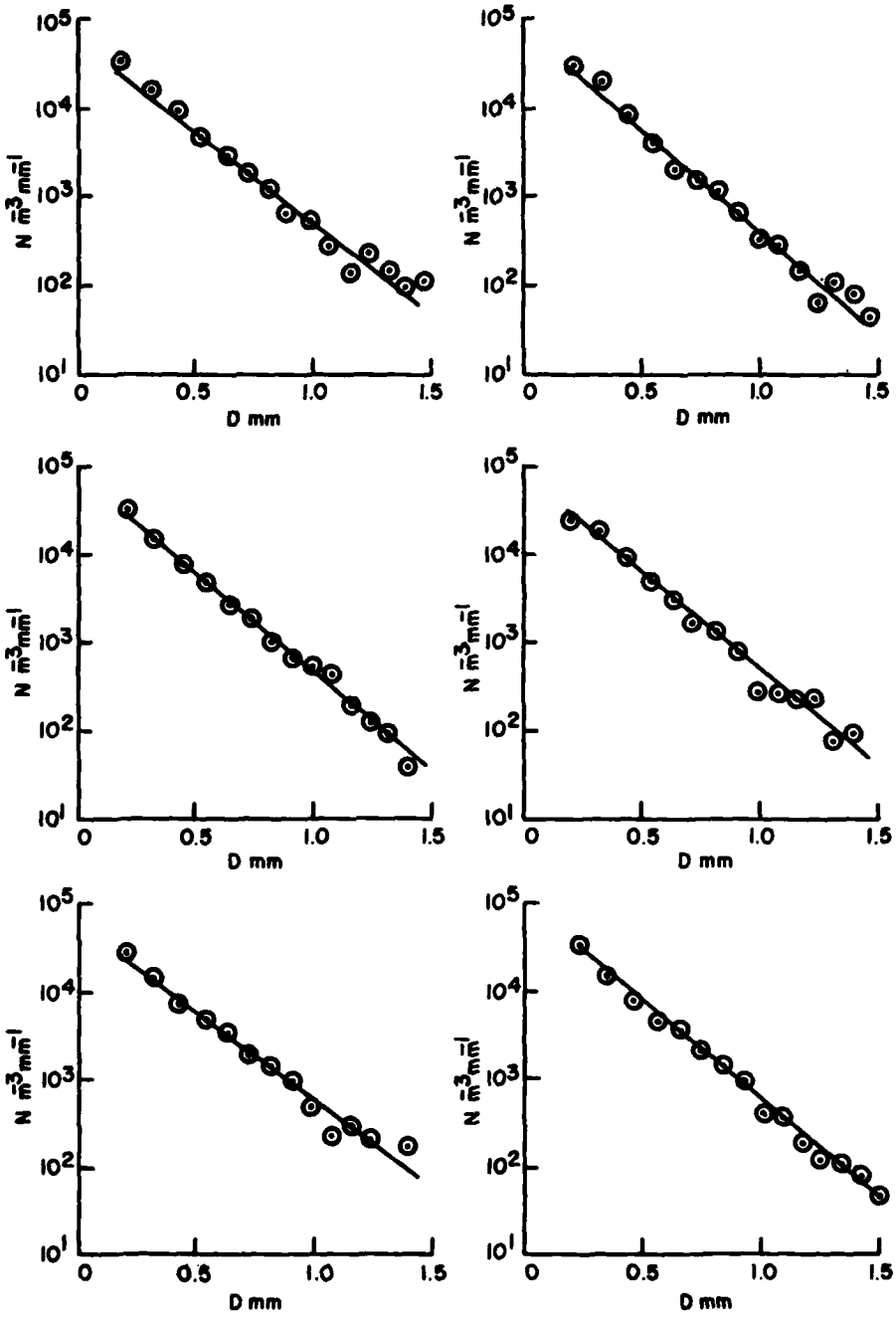

Figure 6. . Six Number-Density Distributions (4-Second Averages) from the Total of 53 from the MC-130E, Pass 5

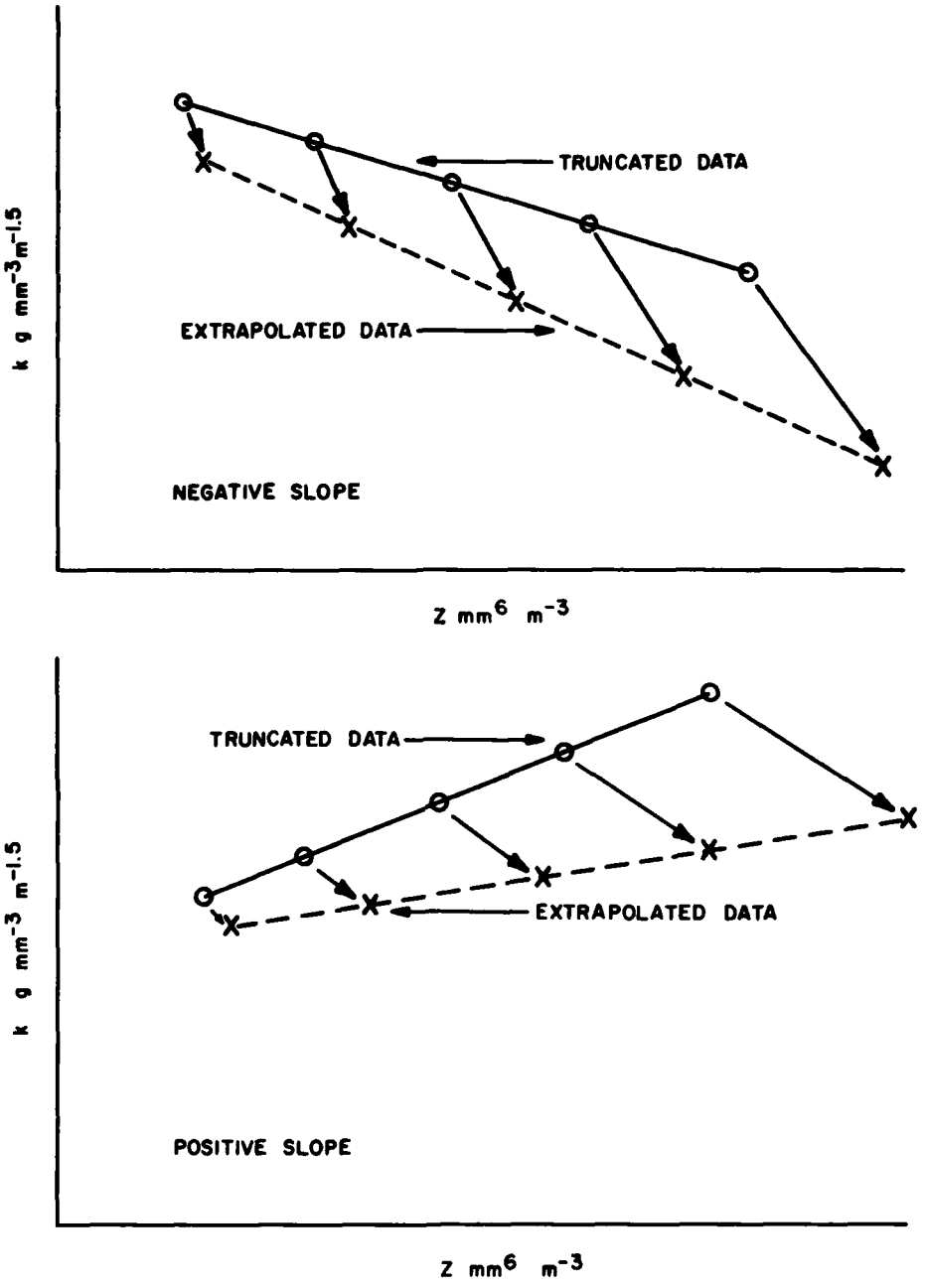

Figure 7. Illustration of the Expected Change in the k_P-Z_P Regression as a Result of Extrapolation

individual distributions. This results in a simpler procedure since a line can be defined by just two points and allows the "best-fit" values of k_P and Z_P from two points on the truncated regression line to be extrapolated to give values of k_E and Z_E. These estimated values, when connected by a straight line on a log-log plot, will give the predicted regression line of the extrapolated data. Thus, for any Z_P there is a corresponding average M_P which can be found using Eq. (33) and then applied to the extrapolation process through Eq. (22) as

$$\Lambda = 61.2 \left(\frac{r_Z}{r_M}\right)^{1/3} \left(\frac{a_2 Z_P^{0.5+b_2}}{Z_P}\right)^{1/3} \quad mm^{-1} \tag{36}$$

M_P can also be found through Eq. (29) as

$$M_P = k\sqrt{Z_P} \quad g\ m^{-3} \tag{37}$$

and can be incorporated into Eq. (22) as

$$\Lambda = 61.2 \left(\frac{r_Z}{r_M}\right)^{1/3} \left(\frac{k}{\sqrt{Z_P}}\right)^{1/3} \quad mm^{-1} \tag{38}$$

The selection of two Z_P's and computation of the corresponding M_P's defines two such conditions (Z_{P1}, M_{P1} and Z_{P2}, M_{P2}) and allows Z_{E1}, M_{E1} and Z_{E2}, M_{E2} to be determined by the extrapolation procedure of Section 2. With these two estimated points, the predicted regression line and the coefficients and exponents of Eqs. (34) and (35) can be determined.

This simplified method was used with the regression values from the original truncated data from the MC-130E, pass 5 where Z_{P1} and Z_{P2} were given the values of plus and minus one standard deviation from the log-average Z of the pass. Table 3 lists the result of this predicated regression in the a and b terms of the power-function equation along with the results from the analysis of the original data and from the extrapolation of each of the 53 individual distributions.

A comparison of the results show that the two methods of estimating the regression of a full distribution agree quite well and indicate that the simplified procedure may be used in place of the longer process with a very slight, acceptable deviation in the a and b terms.

In both of the methods just described, the estimated M_E may be determined for any given Z_E by using Eq. (35) but it may be remembered that if the total M_A is required, the amount measured by the cloud probe (M_C) should be taken into account.

Table 3. Comparison of the a and b Terms of the Power-Function Equation from the Original Data, Extrapolation of Each Separate Distribution and Predicted Regression

	a	b
MC-130E, pass 5 original data	0.08203	-0.2722
Each of the 53 separate distributions extrapolated	0.09111	-0.2944
Predicted regression (Simplified Method)	0.09206	-0.2931

Discussion of the cloud probe data and its combination with that from the precipitation probe is contained in Appendix A.

When a particular hydrometeor environment is measured with both radar and aircraft and the data from the two sources are correlated, then Eq. (30) is used to define the k that is associated with Z_R. In situations where the aircraft measurements are instrumentally truncated, it is the k-parameter only that will be altered by the application of the extrapolation procedure since the Z_R measurements are not subject to the truncation limits of the 1-D instrument. Therefore, the values of Z_R are the actual reflectivity factors from the full distributions. A k_P-Z_R regression line produced through the correlation of truncated aircraft data with radar measured Z_R's will exhibit a different slope than the k_P-Z_P regression line but should change (assuming that Z_E is equal to Z_R), upon extrapolation, to match the slope of the k_E-Z_E regression. (In actual practice, Z_E should not be expected to exactly equal Z_R since both the aircraft and radar measurements contain inherent instrumentation and data-acquisition errors.)

Once again, an illustration may be helpful in visualizing this predicted change. In Figure 8 the diagrams of Figure 7 have been altered to include the k_P-Z_R truncated data points (closed circles) and their direction of change upon extrapolation for regression lines of positive and negative slopes. In both cases, the k_P-Z_R regression lines are closer to a zero slope than their k_P-Z_P counterparts but the most noticeable difference occurs in the amount of change, with the k_P-Z_R line varying more in the negative case and the k_P-Z_P line showing the greatest change in the positive case.

In experimental situations where aircraft and radar data are available and the aircraft values are from truncated measurements, it is required to compensate k_P. In order to incorporate the extrapolation process for the correction of k_P, it is necessary to determine the M_P and Z_P for any given Z_R. This is easily accomplished by forming a new regression of Z_P and Z_R as

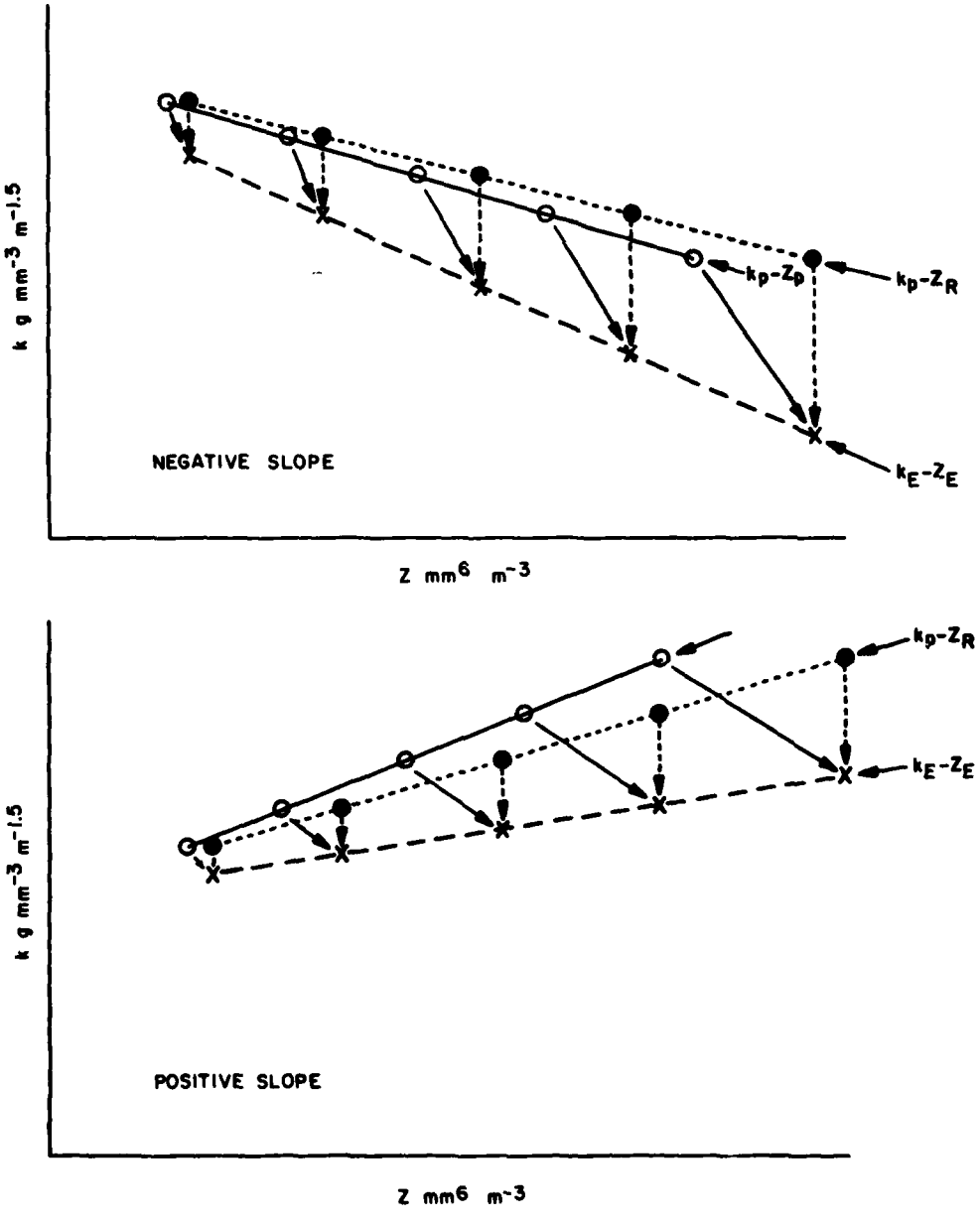

Figure 8. Illustration of the Expected Changes in the k-Z Regression as a Result of Extrapolation

$$Z_P = a_4 \, Z_R^{b_4} \tag{39}$$

which, when substituted in Eq. (29), gives

$$M_P = k_P \left(a_4 \, Z_R^{b_4} \right)^{1/2} \quad g \, m^{-3} \quad . \tag{40}$$

This allows Eq. (22) to be expressed in terms of k_P and Z_R as

$$\Lambda = 61.2 \left(\frac{r_Z}{r_M} \right)^{1/3} \left(\frac{k_P}{\sqrt{a_4 \, Z_R^{b_4}}} \right)^{1/3} \quad mm^{-1} \quad . \tag{41}$$

Using the same technique as in the simplified method of the k_P-Z_P case, two selections of Z may be chosen, this time Z_{R1} and Z_{R2}, and through Eq. (41) and the extrapolation process described in Section 2, two new k_E's can be evaluated. These k_E's, with the selected Z_R's, will give the estimated relationships of the non-truncated spectra with the radar data as

$$k_E = a_5 \, Z_R^{b_5} \tag{42}$$

and

$$M_E = a_5 \, Z_R^{0.5+b_5} \tag{43}$$

The reader is again referred to Appendix A for a discussion on the combination of the cloud and precipitation data.

4. TEST OF THE REGRESSION-PREDICTION METHODS

In Section 2, it was demonstrated than an instrumentally-truncated distribution can be defined by an exponential function when converted into terms of equivalent melted diameters. Therefore, to test the regression-prediction methods outlined in Section 3, exponential distributions (non-instrumentally truncated) may be defined as standards and then truncated, by reduction of the D_M limits, to be made to represent instrumentally truncated aircraft measurements. The values calculated from these truncated situations can then be processed through the previously

described regression-prediction procedures and the results compared with those of the full distributions.

Four exponential distributions were chosen so that they would have differing slopes and that their k and Z points would scatter about, and not fall directly on the regression line. In all of the four cases, the minimum diameter was 0.1 mm and the maximum was 2.6 mm. The parameters of these spectra are listed in Table 4 and their number-density plots are shown in Figure 9.

Table 4. Parameters of the Four Distributions Used to Test the Regression-Prediction Methods

Dist. No.	Λ mm^{-1}	N_o $m^{-3}\,mm^{-1}$	M $g\,m^{-3}$	Z $mm^6\,m^{-3}$	k $g\,mm^{-3}\,m^{-1.5}$	D_M mm
1	4.20	25,000	0.25085	716.783	0.009370	2.6
2	5.75	58,000	0.16617	199.365	0.011769	2.6
3	6.30	31,000	0.06157	56.487	0.008192	2.6
4	8.80	75,000	0.03380	13.213	0.010674	2.6

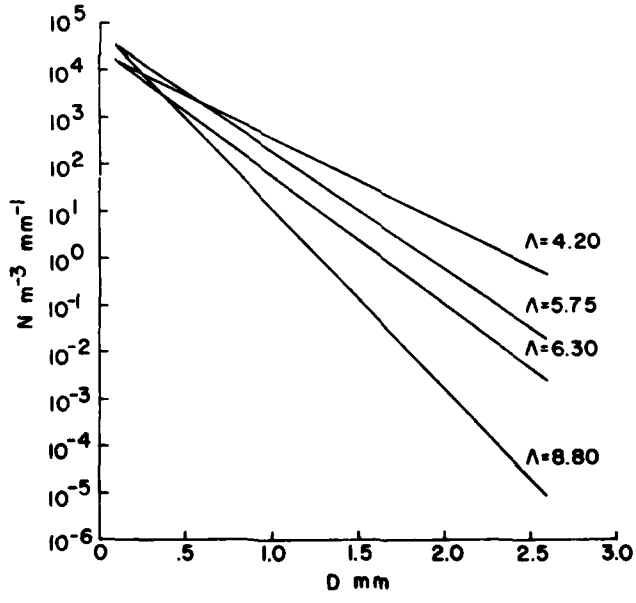

Figure 9. Number-Density Plot of the Four Test Distributions that were Used for the Regression Prediction

When the k's and Z's from Table 4 are subjected to regression analysis as in Figure 10, the power-function equation is $k = 0.010085\ Z^{-0.00379}$ and can be designated as the standard equation to which any predicted regression can be compared. Then each of the test spectrums can be truncated at any diameter (D_T), where D_T is always less than D_M, and the k and Z calculated under this condition will be synonymous with that derived from truncated aircraft data.

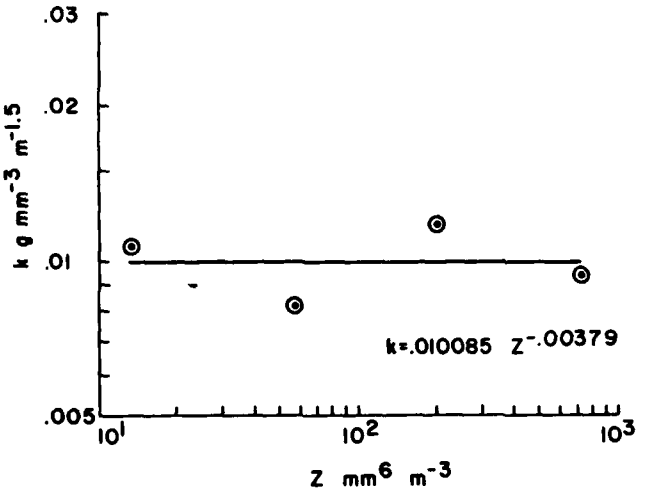

Figure 10. The k-Z_R Regression from the Four Test Distributions

This was done for each of the samples for the D_T limits of 1.0, 1.2, 1.4, 1.6, 1.8, 2.0, 2.2 and 2.4 mm and the resulting k's and Z's are listed in Table 5.

At this point, the simulated aircraft data has been defined and consideration will now be given to the application of these data to the previously outlined methods of predicting the regression equation from the truncated distributions.

The first method discussed in Section 3 was that of aircraft values alone. In this case, the k and Z_A of each distribution, that are the result of a particular truncation limit, were used in a regression analysis to give the relationships of Eqs. (32) and (33). Two Z_A's were then designated as previously described (plus and minus one standard deviation from the log average) and these Z_A's were then applied to Eq. (36) and the extrapolation process of Section 2. The resulting M_E's and Z_E's, one pair for each of the two defined Z_A's, were then used to give the predicted regression lines of the extrapolated data and the coefficients and exponents of the power-function relationship of Eqs. (34) and (35).

Table 5. The Simulated k_A's and Z_A's of the Test Distributions Under Truncated Conditions

D_T mm		Dist. 1	Dist. 2	Dist. 3	Dist. 4
1.0	k g mm^{-3} $m^{-1.5}$ Z mm^6 m^{-3}	0.014979 103.481	0.016258 71.058	0.010745 25.032	0.011830 10.232
1.2	k Z	0.013534 190.266	0.014625 107.564	0.009718 35.698	0.011165 11.910
1.4	k Z	0.012353 292.347	0.013509 139.169	0.009060 43.990	0.010865 12.707
1.6	k Z	0.011427 396.473	0.012781 162.936	0.008660 49.571	0.010742 13.034
1.8	k Z	0.010723 491.889	0.012326 178.930	0.008430 52.942	0.010698 13.154
2.0	k Z	0.010200 572.316	0.012054 188.837	0.008305 54.814	0.010681 13.195
2.2	k Z	0.009822 635.721	0.011899 194.575	0.008239 55.786	0.010676 13.208
2.4	k Z	0.009555 683.042	0.011813 197.719	0.008208 56.263	0.010675 13.211

This procedure was followed in each of the truncated cases and Table 6 lists the coefficients and exponents of the power-function equations for each D_T limit along with those for the standard equation from the full distributions.

The regression lines corresponding to each D_T are plotted in Figure 11 and show the negative change in slope as D_T approaches the D_M limit. (dotted line) Table 7 gives the coefficients and exponents of the predicted regression equations and compares them with those from the standard equation.

It is apparent that there are only very slight differences between the predicted equations and the standard, but since M is the final product, the evaluation can not be considered complete until the M values from the predicted and standard equations are compared. This was done for designated Z's of 10, 100 and 1000 and the results are listed in Table 8.

The second prediction method described in Section 3 was the combination of aircraft and radar data. To test this method, the radar is given the Z values of the non-truncated distributions from Table 4. The truncated aircraft values are, once again, those listed in Table 5.

Table 6. *The Coefficients* and Exponents from the Truncated and Non-Truncated Cases

D_T mm	$k = a_2 Z_A^{b_2}$ --- $M = a_2 Z_A^{0.5+b_2}$		
	a_2	b_2	$0.5 + b_2$
1.0	0.007767	0.14816	0.64816
1.2	0.007891	0.10714	0.60714
1.4	0.008261	0.07440	0.57440
1.6	0.008692	0.04941	0.54941
1.8	0.009100	0.03083	0.53083
2.0	0.009445	0.01734	0.51734
2.2	0.009721	0.00769	0.50769
2.4	0.009932	0.00087	0.50087
D_M 2.6	0.010085	-0.00379	0.49621

Table 7. Predicted Regressions and Their Comparison with the Standard (Simulated Aircraft)

D_T mm	$k_E = a_3 Z_E^{b_3}$ --- $M_E = a_3 Z_E^{0.5+b_3}$			Factor = Predicted / Standard	
	a_3	b_3	$0.5 + b_3$	a	$0.5 + b$
1.0	0.010067	-0.00334	0.49666	0.9982	1.0009
1.2	0.010008	-0.00344	0.49656	0.9924	1.0007
1.4	0.010211	-0.00680	0.49320	1.0125	0.9939
1.6	0.010150	-0.00632	0.49377	1.0064	0.9951
1.8	0.010086	-0.00405	0.49595	1.0000	0.9995
2.0	0.010051	-0.00320	0.49680	0.9966	1.0011
2.2	0.010046	-0.00302	0.49698	0.9961	1.0015
2.4	0.010061	-0.00331	0.49669	0.9976	1.0010
D_M 2.6	0.010085	-0.00379	0.49621	--	--

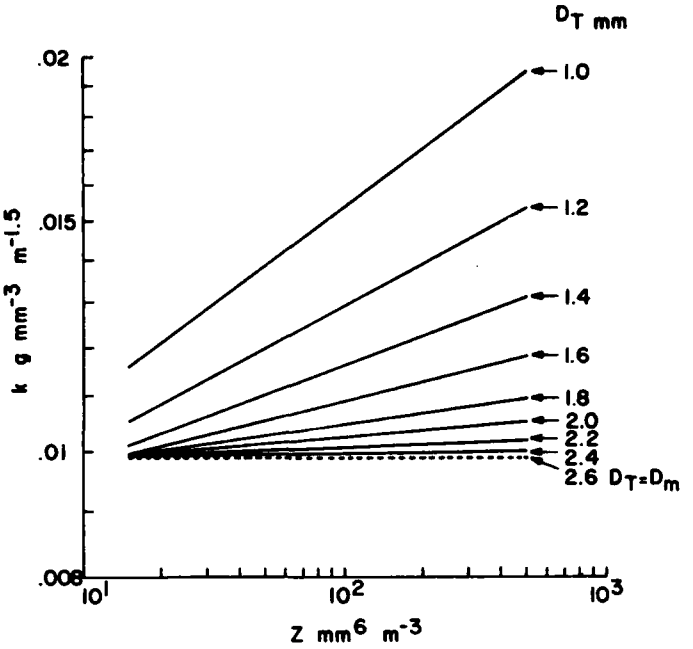

Figure 11. The k-Z_A Regressions from the Four Test Distributions at Various Truncation Limits (D_T)

Table 8. Comparison of M from the Predicted and Standard Equations (Simulated Aircraft). Factor (F) = predicted/standard

	Z = 10 mm^6 m^{-3}		Z = 100 mm^6 m^{-3}		Z = 1000 mm^6 m^{-3}	
D_T mm	M g m^{-3}	F	M g m^{-3}	F	M g m^{-3}	F
1.0	0.031591	0.9993	0.099133	1.0003	0.311086	1.0013
1.2	0.031398	0.9932	0.098507	0.9940	0.309049	0.9948
1.4	0.031788	1.0055	0.098962	0.9986	0.308083	0.9917
1.6	0.031640	1.0008	0.098629	0.9952	0.307451	0.9896
1.8	0.031599	0.9995	0.098996	0.9989	0.310148	0.9983
2.0	0.031550	0.9980	0.099040	0.9993	0.310892	1.0007
2.2	0.031548	0.9979	0.099072	0.9997	0.311124	1.0014
2.4	0.031574	0.9987	0.099088	0.9998	0.310965	1.0009
D_M 2.6	0.031614	--	0.099105	--	0.310675	--

In this method, both the k and Z_A of each distribution, that are the result of a specific truncation limit, are related to the assigned Z_R to give the k-Z_R (Eq. (30)) and Z_A-Z_R (Eq. (39)) regressions. Two Z_R's are then designated (once again, plus and minus one standard deviation from the log average) and the k's associated with the two Z_R values are determined for the specified D_T limit. Substituting the two Z_R's and their associated k's in Eq. (41) then allows two estimated M_E (or k_E) and Z_E pairs to be calculated through the extrapolation process of Section 2. The plotting of the logarithmic values of these estimated points will give the predicted regression line.

This procedure was followed for each of the truncated situations and the coefficient and exponents of the k-Z_R and Z_A-Z_R relationships are listed in Table 9.

Table 9. The Coefficients and Exponents of the k-Z_R and Z_A-Z_R Regressions

D_T mm	$k = a_1 Z_R^{b_1}$		$Z_A = a_4 Z_R^{b_4}$	
	a_1	b_1	a_4	b_4
1.0	0.009023	0.08338	2.27332	0.60392
1.2	0.008646	0.07284	2.02020	0.71226
1.4	0.008682	0.05745	1.72348	0.79862
1.6	0.008911	0.04152	1.47858	0.86462
1.8	0.009209	0.02734	1.29992	0.91327
2.0	0.009497	0.01586	1.17622	0.94807
2.2	0.009744	0.00711	1.09254	0.97235
2.4	0.009941	0.00069	1.03664	0.98893

The predicted regressions are given in Table 10 where they are compared with the standard equation.

Once again, the more significant comparison of M's from the predicted and standard equations are given in Table 11.

It is evident, that the factors in the radar-aircraft case have a slightly larger variance than that of the aircraft-only method, although both are able to estimate the standard regression equation to within a very close tolerance.

Table 10. Predicted Regressions and Their Comparison with the Standard (Simulated Aircraft and Radar)

D_T mm	$k_E = a_5 Z_R^{b_5}$ --- $M_E = a_5 Z_R^{0.5+b_5}$			Factor = Predicted / Standard	
	a_5	b_5	$0.5 + b_5$	a	0.5 + b
1.0	0.010462	-0.01184	0.48816	1.0374	0.9838
1.2	0.010420	-0.01112	0.48888	1.0332	0.9852
1.4	0.010321	-0.00913	0.49087	1.0234	0.9892
1.6	0.010208	-0.00676	0.49324	1.0122	0.9940
1.8	0.010127	-0.00494	0.49506	1.0042	0.9977
2.0	0.010079	-0.00380	0.49620	0.9994	1.0000
2.2	0.010063	-0.00339	0.49661	0.9978	1.0008
2.4	0.010068	-0.00344	0.49656	0.9983	1.0007
D_M 2.6	0.010085	-0.00379	0.49621	--	--

Table 11. Comparison of M from the Predicted and Standard Equations (Simulated Aircraft and Radar). Factory (F) = predicted/standard

D_T mm	Z = 10 $mm^6 m^{-3}$		Z = 100 $mm^6 m^{-3}$		Z = 1000 $mm^6 m^{-3}$	
	M g m^{-3}	F	M g m^{-3}	F	M g m^{-3}	F
1.0	0.032194	1.0183	0.099068	0.9996	0.304856	0.9813
1.2	0.032118	1.0159	0.098998	0.9989	0.305146	0.9822
1.4	0.031959	1.0109	0.098960	0.9985	0.306430	0.9863
1.6	0.031782	1.0053	0.098951	0.9984	0.308078	0.9916
1.8	0.031662	1.0015	0.098992	0.9989	0.309500	0.9962
2.0	0.031595	0.9994	0.099042	0.9994	0.310468	0.9993
2.2	0.031575	0.9988	0.099071	0.9997	0.310855	1.0006
2.4	0.031866	0.9991	0.099098	0.9999	0.310902	1.0007
D_M 2.6	0.031614	--	0.099105	--	0.310675	--

5. REAL-TIME ESTIMATIONS FROM TRUNCATED DISTRIBUTION DATA

Real-time analysis of the 1-D data is very important to the meteorologist on board the sampling aircraft and also, through a radio link, to the ground-based mission control. Knowledge of liquid water content can be particularly critical in some situations especially in the lower altitudes of a storm where snow crystals are large and truncation effects are most likely to occur.

Both the Lear and the MC-130E have on-board computers which give the field personnel real-time parameters of the hydrometeor environment in which they are sampling. However, when the aircraft passes through a region containing large-size particles the calculated results reflect the conditions of truncated spectra and not the true situation of the full actual distributions. It is at this point that quick, yet reasonably accurate estimates of the true M and Z are needed.

It is a relatively simple matter to instruct the computers to recognize a probable truncated situation since this possibility could exist whenever the largest diameter-size channel of the precipitation probe has recorded counts. But, it is not feasible to have these computers extrapolate distributions because of their limited capacity.

Therefore, equations have been derived to give an approximation of the M_E and Z_E that would be obtained through the extrapolation of a truncated distribution using as input the real-time calculations of M_P and Z_P. These equations are based on exponential distributions that have upper and lower diameter limits corresponding to those of the precipitation probes on the aircraft. They were developed using a process of plotting variations of M_P/Z_P vs M_E/Z_E until a very near straight-line relationship existed and then were converted into equation form.

A large-snow crystal type was assumed where $\alpha = 0.4$ and $\beta = 0.782$ in Eq. (4) and the extrapolation limit was set at $D_M\Lambda = 9$.

The equations for large snow conditions using the Lear probe are

$$M_E = M_P \left[e^{2303 \left(\ln \frac{M_P \times 10^4}{Z_P} \right)^{-9.5155} - 0.02} \right] \tag{44}$$

and

$$Z_E = Z_P \left[e^{394.3 \left(\ln \frac{M_P \times 10^4}{Z_P} \right)^{-6.1093} - 0.25} \right] . \tag{45}$$

The corresponding equations to be used with the probe on the MC-130E are

$$M_E = M_P \left[e^{4.6657} \left(\ln \frac{M_P \times 10^4}{Z_P} \right)^{-5.714} - 0.02 \right] \tag{46}$$

and

$$Z_E = Z_P \left[e^{9.5086} \left(\ln \frac{M_P \times 10^4}{Z_P} \right)^{-4.1663} - 0.25 \right] . \tag{47}$$

Both sets of equations are of the same form with the exponents reflecting the differences in the upper truncation limits of the two different 1-D precipitation probes.

It should be emphasized, that these equations have been developed to give a quick method of estimating the M and Z from a single distribution (that is, aircraft data averaged over any length of time into a single distribution) and should not be confused with the more precise post-mission, multi-sample regression analysis.

The M_P's and Z_P's from the sample distributions presented in Section 2 were substituted in these equations and the results are listed in Table 12.

Table 12. Comparison of M_E and Z_E from Extrapolation and Real-Time Equations

	Real-Time		Extrapolated		Factor $\left(\frac{\text{Real-Time}}{\text{Extrapolated}}\right)$	
	M_E g m^{-3}	Z_E mm^6 m^{-3}	M_E g m^{-3}	Z_E mm^6 m^{-3}	for M_E	for Z_E
Lear	0.3509	268.5	0.3533	268.3	0.993	1.001
MC-130E Pass 3	0.4162	844.2	0.4144	845.5	1.004	0.998
MC-130E Pass 5	0.3159	393.4	0.3137	393.6	1.007	1.000

Further comparisons of M_E and Z_E were made between the results of the real-time calculations and the extrapolation process using a variety of M_P's and Z_P's. It was found, through this testing, that if the M_E or Z_E were less than

twice the value of M_P or Z_P, then the estimated results from the two methods differed less than 1 percent. In other words, if the estimated M were within a factor of 2 from M_P then the results calculated by either method fall within 1 percent of each other. The same rules apply for Z_P and Z_E.

When the tests were compared at a factor of 3 increase in the estimated values, the differences were within 5 percent.

As a final word, it must be remembered that the subscripted "P" and "E" values refer to the measured and estimated data of the precipitation probe and that the M_C and Z_C from the cloud probe must be added to the estimated values to obtain a total M_A and Z_A.

6. CONCLUSIONS

The analytical processes presented in this report are the results of a study conducted on truncated measurements from aircraft (PMS 1-D) instruments. A method of extrapolating these truncated data is demonstrated and the procedure whereby the extrapolated data are conveniently used in a regression analysis is described.

Testing of these processes have indicated that this extrapolation method can be considered valid if the assumptions of an exponential number-density distribution and a D_M upper limit, as determined by the equation $D_M\Lambda = C$, are accepted as a reasonably accurate description of reality for the majority of cases, However, it must be emphasized that not all samples will have distributions that are able to be described by an exponential function. An occasional pass will have an excess or a deficiency of specific size particles which result in number-density distributions that depart from exponential. Also the $D_M\Lambda$ constant of 9 used in this report is specific for the ice hydrometeors that were measured in a particular storm and can vary with crystal shape and density. Past AFGL measurements have indicated a $D_M\Lambda$ constant within the range of 9 to 12.

Instruments of the future may prove or disprove these assumptions and may, ideally, negate the need of extrapolating, but further study is needed to related maximum particle crystal size, through t to D conversion, to a D_M limit until such instruments are developed and put into operation. A better knowledge of the $D_M\Lambda$ constant and the α and β of the t to D equation should enable the exponential-distribution equations to be fine-tuned to more accurately describe the various snow types as to their density and size.

Although the described extrapolation method deals exclusively with ice hydrometeors, it can also be applied in cases of truncated distributions in rain. The Lear 1-D, for example, has a maximum measuring size of 3.105 mm for water

drops and can be expected to encounter situations having hydrometeors of some larger size. In cases involving liquid water there is no t to D considerations and the only change in the analytical procedure would be in the $D_M\Lambda$ constant. For rain, this constant is given the value of 7.5 up to an absolute maximum of 5 mm which is considered to be the breakup size of a water drop.

It is recommended that the methods outlined in this report be incorporated in the analyses of PMS aircraft data and that the real-time equations be programmed into aircraft computers so that full utilization may be made of the instrumentally truncated data.

References

1. Barnes, A.A., Jr. (1978) New cloud physics instrumentation requirements, Preprints, Fourth Symposium on Meteorological Observations and Instrumentation, American Meteorological Society, 264-268, AFGL-TR-78-0093, AD A053 235.

2. Knollenberg, R.G. (1970) The optical array: an alternative to scattering or extinction for airborne particle size determination, J. Appl. Meteor. Vol. 9, No. 1, pp 86-103.

3. Knollenberg, R.G. (1976) Three new instruments for cloud physics measurements: The 2-D spectrometer, the forward scattering spectrometer probe and the active scattering aerosol spectrometer, Am. Meteor. Society International Conference on Cloud Physics, July 26-30, 1976, Boulder, Colorado, Preprint Vol. pp 554-561.

4. Cunningham, R.M. (1978) Analysis of particle spectral data from optical array (PMS) 1-D and 2-D sensors, Fourth Symposium on Meteorological Observations and Instrumentation, April 10-14, 1978, Denver, Colorado, Preprint Vol., pp 345-350.

5. Gunn, K.L.S., and Marshall, J.S. (1958) The distribution with size of aggregate snowflakes, J. Meteorol. 15:452(479).

6. Marshall, J.S., and Palmer, W.McK. (1948) The distribution of raindrops with size, J. Meteorol. 5:165-166.

7. Marshall, J.S., and Gunn, K.L.S. (1952) Measurement of snow parameters by radar, J. Meteorol. 9:322.

8. Plank, V.G. (1974) Hydrometeor parameters determined from the radar data of the SAMS Rain Erosion Program, Environmental Research Papers, No. 477, AFCRL/SAMS Report No. 2, AFCRL-TR-74-0249, AD 786 454, 86 pp.

9. Plank, V.G. (1977) Hydrometeor data and analytical-theoretical investigations pertaining to the SAMS Missile Flights of the 1972-73 season at Wallops Island, Virginia, Environmental Research Papers, No. 603, AFGL/SAMS Report No. 5, AFGL-TR-77-0149, AD A051 192, 239 pp.

10. Sekhon, R.S., and Srivastava, R.C. (1970) Snow size spectra and radar reflectivity, J. Atmos. Sci. 27:299-307.

11. Church, J.F., Pocs, K.K., and Spatola, A.A. (1975) The Continuous Aluminum Foil Sampler; design operation, data analysis procedures, and operating instructions, Instrumentation Papers, No. 235, AFCRL-TR-75-0370, AD A019 630, 70 pp.

12. Barnes, A.A., Nelson, L.D., and Metcalf, J.I. (1974) Weather documentation at Kwajalein Missile Range, 6th Conference on Aerospace and Aeronautical Meteorology, American Meteorological Society, 66-69, Air Force Surveys in Geophysics, No. 292, AFCRL-TR-74-0430, AD A000 925, 14 pp.

13. Barnes, A.A., Metcalf, J.I., and Nelson, L.D. (1974) Aircraft and radar weather data analysis for PVM-5, Air Force Surveys in Geophysics, No. 297, AFCRL/Minuteman Report No. 1, AFCRL-74-0627, AD B004 290, 47 pp.

14. Plank, V.G. (1974) A summary of the radar equations and measurement techniques used in the SAMS Rain Erosion Program at Wallops Island, Virginia, Special Reports, No. 172, AFCRL/SAMS Report No. 1, AFCRL-TR-74-0053, AD 778 095, 108 pp.

15. Plank, V.G. (1974) Liquid-water-content and hydrometeor size-distribution information for the SAMS Missile Flights of the 1971-72 season at Wallops Island, Virginia, Special Reports, No. 178, AFCRL/SAMS Report No. 3, AFCRL-TR-74-0296, AD A002 370, 143 pp.

16. Plank, V.G., and Barnes, A.A. (1978) An improvement in obtaining real-time water content values from radar reflectivity, AMS 18th Conference on Radar Meteorology, March 28-31, 1978, Atlanta, GA, Preprint Vol., pp 426-431.

Appendix A

The Combining of the Cloud and Precipitation Probe Data

The extrapolation process described in this report is concerned only with the number-density spectra from truncated distributions as measured with the 1-D precipitation probe. Any estimated values determined through the use of this method may be supplemented with the data from the cloud probe in order to define the parameters of a total spectrum measured over the range of both instruments.

Unlike the precipitation probes, the cloud 1-D's are identical on both aircraft with each being capable of measuring snow crystals from 0.015 to 0.360 mm. Since the smallest measurable sizes of the precipitation probes are 0.151 mm for the Lear and 0.227 mm for the MC-130E, it is evident that an overlap occurs in the measurements when using data from both the cloud and precipitation probes. Fortunately, the redundant spectra can be conveniently eliminated by considering just the cloud instrument data for all sizes up to that which corresponds to the lower limit of the precipitation probe. For example, on the Lear, the upper limit of channel 6 of the cloud probe is 0.153 mm and when compared to the lower limit of 0.151 mm of the precipitation probe, shows a slight overlap of 0.002 mm. Channel 10 of the cloud probe has an upper limit of 0.222 mm and when compared with the lower limit of 0.227 mm of the MC-130E precipitation probe shows that a 0.005 mm segment is missed. These errors are minor and can be safely ignored.

In the following discussion, all references to cloud probe data assume that these data have been limited in accordance with the above rules.

Table 1 lists the M and Z contributions from the cloud and precipitation probes for the three sample truncated distributions. It is evident from these data that when extrapolation of the data is required, the combined cloud and precipitation measurements need only be considered for the M parameter since the cloud Z-contributions are 0.01 percent or less of the total. In some cases, which depend entirely upon the proposed use of the data, even the ~6 to 7 percent M contribution may be of such little importance that it too, may be ignored.

The combining of the data from the two size ranges is simple and straightforward when considering a single distribution. In this instance, the M_C is added directly to the M_P or M_E to give the total M_A as

$$M_A = M_C + M_{(P \text{ or } E)} \tag{A1}$$

When two or more distributions are used to form a k_P-Z_P regression any averaged value of Z_P will not only have an average M_P but also an average M_C associated with it. This M_C can be determined by forming a relationship between the M_C and Z_P from the experimental data as

$$M_C = x\, Z_P^y \tag{A2}$$

When the Z_P is replaced by Z_E through the extrapolation process then a new relationship can be formed.

$$M_C = x_1\, Z_E^{y_1} \tag{A3}$$

The M_C determined in Eq. (A3) can then be substituted in Eq. (A1) to find M_A.

Radar Z's can be directly associated with M_C as

$$M_C = x_2\, Z_R^{y_2} \tag{A4}$$

where the M_C is then used in Eq. (A1).

An alternative, that may be used to avoid these regressions, is to use the pass-averaged M_C in Eq. (A1). Since the percentage of the averaged M_C is small, when compared with the pass-averaged total M_A, the discrepancies caused by the direct addition of the mean M_C with M_P are insignificant.

These two methods of combining the cloud and precipitation data were explored using the experimental results of the MC-130E, pass 5 (Table 1, Figures 3 and 4). This pass has the largest contribution of M_C (7.4 percent) of all three samples listed in Table 1.

The M_C and Z_P values for the 53 distributions were analyzed and gave the relationship of $M_C = 0.05569\ Z_P^{-0.1416}$. The maximum Z_P of the pass was 638.6 and the minimum was 174.2 and when applied to the M_C-Z_P equation, give M_C's of 0.0223 for the maximum Z_P and 0.0268 for the minimum.

The equation from the precipitation probe data (Figure 4) was $k_P = 0.08203\ Z_P^{-0.2722}$ and when converted to the M-Z form of Eq. (33), gives an M_P of 0.3573 for the maximum Z_P and 0.2658 for the minimum.

Combining the M_P's with the M_C's from the regression method yields M_A's of 0.3796 for the Z_P maximum case and 0.2926 for the minimum. The pass-averaged method gives 0.3827 and 0.2912 respectively and differs from the regression values by less than 1 percent.

These small variations justify the use of the pass-averaged values of M_C in the computation of total, estimated M when extrapolation of the spectra above the upper limit of the 1-D precipitation probe is required.

Appendix B

List of Symbols

a	power-function coefficient
b	power-function exponent
C	constant
d	minimum drop or equivalent melted diameter
D_i	drop or equivalent melted diameter of classified data
D_M	maximum drop or equivalent melted diameter
D_T	drop or equivalent melted diameter at truncation limit
k	aircraft spectral parameter
k_E	estimated spectral parameter
l	measured physical size of ice hydrometeors
M	liquid or ice water content
M_A	liquid or ice water content from aircraft data
M_C	liquid or ice water content derived from cloud probe
M_D	liquid or ice water content at drop or equivalent melted diameter D
M_E	estimated liquid or ice water content from an extrapolated distribution
M_P	liquid or ice water content derived from precipitation probe

ΔM	liquid or ice water content from the extrapolated part of the distribution
N	number concentration of the hydrometeor drops or particles per m^3 per mm bandwidth
N_D	number concentration at diameter D
N_i	number concentration for classified data
N_o	the "zero intercept" of a distribution function of exponential type
N_T	total number of the hydrometeor drops of particles of a given population, per m^3
r_M	truncation ratio of liquid water content
r_N	truncation ratio of number concentration
r_Z	truncation ratio of radar-reflectivity factor
Z	radar-reflectivity factor
Z_A	radar-reflectivity factor computer from aircraft data
Z_C	radar-reflectivity factor from cloud probe
Z_D	radar-reflectivity factor at diameter D
Z_E	estimated radar-reflectivity factor from an extrapolated distribution
Z_P	radar-reflectivity factor from precipitation probe
Z_R	radar-reflectivity factor as measured by radar
ΔZ	radar-reflectivity factor from the extrapolated part of the distribution
α	coefficient of the I to D equation
β	exponent of the I to D equation
$\Gamma(n)$	gamma function of the particular number "n"
Λ	exponential "slope factor" in the distribution function for the number concentration of the drops or particles
ρ_w	density of liquid water

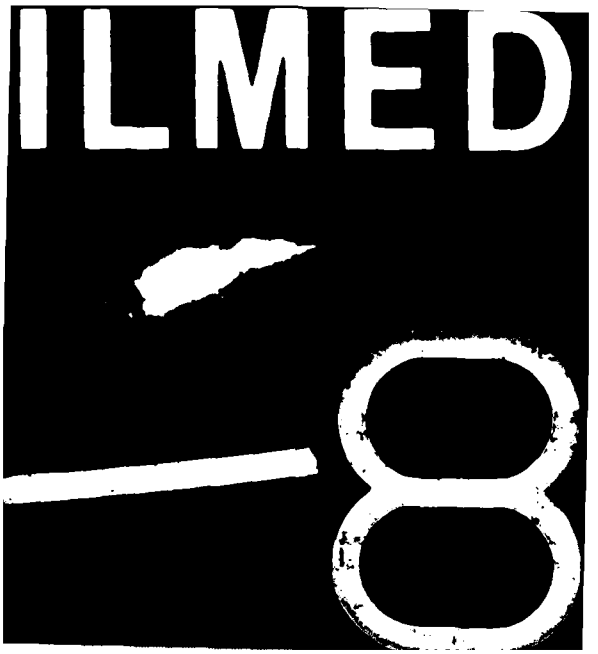
ILMED
8